

DNA Structures

DOI: 10.1002/ange.200503114

Diagnostics of Single Base-Mismatch DNA Hybridization on Gold Nanoparticles by Using the Hyper-Rayleigh Scattering Technique**

Paresh Chandra Ray*

The integration of nanotechnology with biology and medicine is expected to produce major advances in molecular diagnostics, therapeutics, and bioengineering.^[1a-p] Detection of specific DNA sequences has important applications in clinical diagnosis, the food and drug industry, pathology, genetics, and environmental monitoring. The increasing availability of nanostructures with highly controlled optical properties in the nanometer-size range has created widespread interest in their use in biotechnological systems for diagnostic applications and biological imaging. Most assays identify specific sequences through the hybridization of an immobilized probe to the target analyte after the latter has been modified with a fluorescent or Raman tag. Diagnostics of oligonucleotide sequences by using unmodified DNA remains attractive owing to simplified sample preparation, decreased assay costs, and the elimination of potential artifacts from modification. Herein, we demonstrate for the first time that the hyper-Rayleigh scattering (HRS) technique,^[2a-e, 3a-e, 4a-c] which has emerged over the past decade as a powerful method to determine the microscopic nonlinear optical (NLO) properties of species in solution, can be used to achieve the ultrasensitive detection of single base-pair mismatches in oligonucleotide strands without any modification of DNA. The HRS or nonlinear light scattering can be observed from fluctuations in symmetry, caused by rotational fluctuations. A solution is only centrosymmetric on average in time and space. Locally, deviations from centrosymmetry occur and

give rise to a second-order NLO response. Hence, scattering by a fundamental laser beam can be detected at the second harmonic wavelength. The HRS technique can be easily applied to study a very wide range of materials because electrostatic fields and phase matching are not required. The HRS technique is 1–2 orders of magnitude more sensitive than the usual colorimetric technique. Vance et al.^[2a] have shown that the HRS intensity was enhanced by a factor of up to 10^5 in suspensions of nanocrystalline gold particles. Although HRS spectroscopy has been shown^[2a-e] to be capable for the ultrasensitive detection of nanoparticle aggregation, second-order nonlinear spectroscopy remains unexplored for DNA-detection purposes.

Oligonucleotides with different chain lengths, for example, 1) GGCCCCAAACCTTTTGAAAGGACCC-3', 2) GGCCAAAACCTGGAGG-3', 3) GGCAACCT-3' and their complement and noncomplements (one base-pair mismatch) were purchased from MWG Biotech. Hydrogen tetrachloroaurate ($\text{HAuCl}_4 \cdot 3\text{H}_2\text{O}$), phosphate-buffered solution (PBS), sodium chloride, and sodium citrate were purchased from Sigma-Aldrich and used without further purification. The HRS technique^[3a-e] is based on light scattering—linear light scattering is caused by refractive-index variations—and the typical HRS experimental setup that was used in this project has been described previously.^[3a-e] In brief, a Q-switched Nd:YAG laser (Spectra Physics) that delivers 8 ns pulses and up to 800 mJ per pulse at 1064 nm was used as a laser source. To avoid multiphoton photoluminescence contribution, an optical parametric oscillator was used to generate the 1300 nm fundamental wavelength so that the second harmonic is out of an absorption band for the gold-coated DNA. Figure 1 shows the output signal intensities

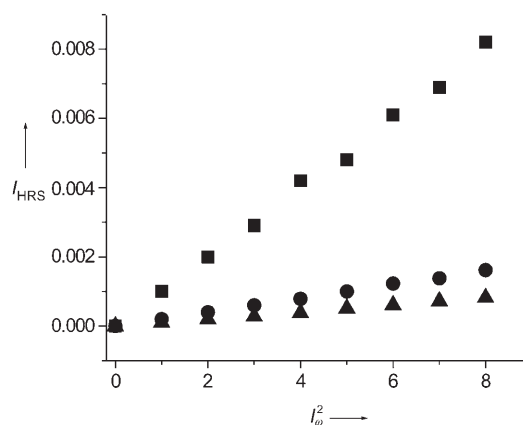


Figure 1. Power dependence of HRS intensity at different concentrations of ss-DNA (GGCAACCTGAGGACCC-3') adsorbed on gold nanoparticles. Squares: $3 \times 10^{16} \text{ cm}^{-3}$; circles: $6 \times 10^{15} \text{ cm}^{-3}$; triangles: $4 \times 10^{15} \text{ cm}^{-3}$.

at 650 nm from single-stranded DNA (ss-DNA) adsorbed onto gold nanoparticles at different powers of 1300 nm incident light. The linear nature of the plot implies that the doubled light is indeed due to the HRS signal. The intensity (I_{HRS}) of the hyper-Rayleigh signal from an aqueous solution

[*] Prof. Dr. P. C. Ray
Department of Chemistry
Jackson State University
1400 J. R. Lynch Street, Jackson, MS 39217 (USA)
Fax: (+1) 601-979-3674
E-mail: paresh.c.ray@jsums.edu

[**] P.C.R. thanks the NSF-CRIF:MU (grant number 0443547) and the NIH-RCMI (grant number G12RR13459) for their generous funding, and the reviewers whose valuable suggestions improved the quality of this manuscript.

of gold nanoparticles can be expressed as shown in [Eq. (1)],

$$I_{\text{HRS}} = G(N_w \beta_w^2 + N_{\text{nano}} \beta_{\text{nano}}^2) I_w^2 e^{-N_{\text{nano}} \epsilon_{2\omega} l} \quad (1)$$

where G is a geometric factor, N_w and N_{nano} are the number of water molecules and gold nanoparticles per unit volume, respectively, β_w and β_{nano} are the quadratic hyperpolarizabilities of a single water molecule and a single gold nanoparticle, respectively, $\epsilon_{2\omega}$ is the molar extinction coefficient of the gold nanoparticle at 2ω , l is the path length, and I_w the fundamental intensity. The exponential factor accounts for the losses through absorption at the harmonic frequency.

The HRS signal intensities were normalized to the square of the fundamental beam power. To extract absolute values for the hyperpolarizabilities, the intensities were normalized again with *para*-nitroaniline (pNA) in methanol. The measured hyperpolarizability for pNA was 34.6×10^{-30} esu at 1064 nm excitation, which is in complete agreement with the reported values^[3b-c] and 25.6×10^{-30} esu at 1300 nm excitation. Through the use of $\beta_w = 0.56 \times 10^{-30}$ esu, as reported in the literature, we have found that $\beta_{\text{nano}} = 4.5 \times 10^{-26}$ esu for 13-nm gold nanoparticles and 4.8×10^{-26} esu for DNA-adsorbed gold nanoparticles, which is much higher than the β values reported for the best available molecular chromophores.

The HRS response from spherical particles has two origins. The first one is a surface contribution that arises from the breaking of centrosymmetry at the particle surface. Because the particle diameter is much smaller than the wavelength of incident light, it is always possible to find a surface element opposite to the surface element of consideration with an inverted orientation of its nonlinear polarization. The second-harmonic light emitted from the surface of the sphere only originates from a nonlocally excited effective electric dipole and a locally excited effective electric quadrupole. As a result, the SH signal intensity scales with the sixth power of the particle radius and may be resonantly enhanced when the dipolar or the quadrupolar mode of the local field is excited at either the fundamental or the harmonic frequency. The second contribution is owing to the bulk contribution that arises from the electromagnetic-field gradients due to the presence of the interface. This contribution extends to over several nanometers away from the interface. Figure 2 shows how the HRS intensity varies after the addition of target DNA into probe DNA (GGCAACCTGAGGACCC-3'; 50 nm). We observed a very distinct HRS intensity change after hybridization even at the concentration of 10 nM probe ss-DNA. The HRS intensity did not change when we added the target DNA with one base-pair mismatch with respect to the probe DNA. One can note that although the visible color changes (as shown in Scheme 1) can be observed only after addition of 250 nm complementary DNA, the HRS signal change can be observed even after addition of complementary DNA (10 nM).

The HRS intensity change is mainly owing to two factors. First, when target DNA with a complementary sequence is added to the probe DNA, a clear colorimetric change from red to blue-gray is observed as shown in Scheme 1. This is owing to the fact that in the presence of ss-DNA, the oligonucleotides adsorb onto the gold colloid through van der

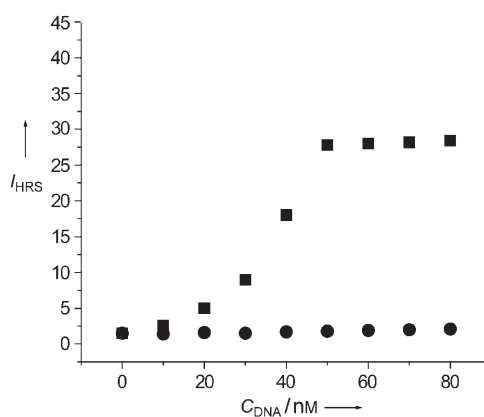
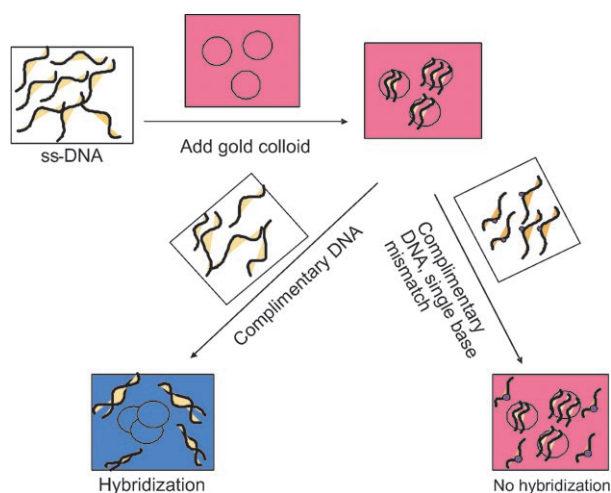


Figure 2. Plot of HRS intensity versus concentration of target DNA. Squares: target DNA; circles: target DNA with one base-pair mismatch.



Scheme 1. Schematic representation of the DNA-hybridization process. The circles represent colloidal gold nanoparticles. Dots in ss-DNA represent one base-pair mismatch

Waals electrostatic forces and provide negative charges that enhance the repulsion between the gold nanoparticles. The electrostatic forces are due to dipolar interactions and depend on the configuration and orientation of the ss-DNA. As transient structural fluctuations permit short segments of the ss-DNA to uncoil, the bases face the gold nanoparticle. Attractive electrostatic forces between the gold nanoparticles and nucleotides cause the ss-DNA to adsorb onto the gold colloid. After hybridization, ss-DNA forms ds-DNA (double-stranded DNA) that has double-helix geometry. As a result, the ds-DNA cannot uncoil sufficiently (unlike ss-DNA) to expose its bases toward the gold nanoparticle. Repulsion between the charged phosphate backbone of ds-DNA and the citrate ions from the gold nanoparticle dominates the electrostatic interaction and does not allow the ds-DNA to adsorb onto the gold nanoparticle. As a result, gold nanoparticles undergo aggregation owing to the presence of NaCl (as shown in Scheme 1).

A two-level model that has been extensively used for donor–acceptor NLO chromophores can be used to explain

the difference in first-order nonlinearity owing to the change in color of nanoparticles. According to the two-state model [Eq. (2)],^[5] where μ_{eg} is the transition dipole moment between

$$\beta^{\text{two state}} = \frac{3\mu_{eg}^2 \delta\mu_{eg}}{E_{eg}^2} \frac{\omega_{eg}^2}{(1-4\omega^2/\omega_{eg}^2)(\omega_{eg}^2-\omega^2)} \quad (2)$$

static factor dispersion factor

the ground state $|g\rangle$ and the charge-transfer excited state $|e\rangle$, $\Delta\mu_{eg}$ is the difference in dipole moment, and E_{10} is the transition energy.

As the color changed from red to blue-gray, the λ_{max} changed from 520 nm to 640 nm and β changed tremendously. This is owing to the fact that at the laser wavelength of 1300 nm and a λ_{max} of 520 nm, there is a small two-photon resonance enhancement (factor of 3.31). For the λ_{max} at 640 nm, however, this resonance enhancement factor is much larger (factor of 43) owing to the closeness of λ_{max} with the second-harmonic wavelength at 650 nm.

Second, after hybridization, the gold nanoparticles undergo aggregation and the HRS intensity increases tremendously with the increase in particle size. Figure 3 shows

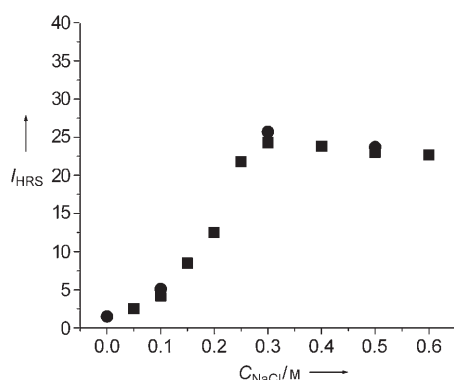


Figure 3. Plot of HRS intensity from gold nanoparticles versus different concentrations of NaCl. Squares: gold nanoparticles; circles: probe DNA adsorbed gold nanoparticles after hybridization.

how the HRS intensity increases with the particle size of gold aggregates by varying NaCl concentration. The HRS intensity was enhanced by a factor of 20 as compared to the HRS signal of the pure gold solution which was decreased slightly and then finally saturated at higher NaCl concentrations. The enhancement factor after hybridization is about the same for pure and DNA-adsorbed gold nanoparticles. To understand the limitation of HRS assays on long target DNA sequences, we have performed our experiment by using 8-, 16-, 25-, 45-, 65-, and 75-base oligonucleotides. Our results indicate that the HRS assay can be easily used to probe longer oligonucleotides (< 75 bases), with the only limitation being that the hybridization process is slow owing to the adsorption process of long ss-DNA sequences on gold nanoparticles.

In summary, we have demonstrated that the HRS assay for ss-DNA sequence recognition at the 10-nanomolar level is based on the differences in electrostatic properties between

ss-DNA and ds-DNA. Our experimental results reported herein open up the new possibility of rapid, easy, and reliable diagnosis of single base-mismatch DNA by measuring the HRS intensity from DNA-modified gold nanoparticles. This method has several advantages: 1) unmodified protein and DNA can be used to probe single base-mismatch DNA in solution by the HRS technique, 2) it can be 1–2 orders of magnitude more sensitive than the usual colorimetric technique, and 3) single base-pair mismatches are easily detected. For the development of practical bioassays, much more research needs to be done on the improvement of the HRS experimental system and the variation of the HRS intensity with the shape and size of metal nanoparticles should also be investigated. It is probably possible to improve the HRS intensity by several orders of magnitude by choosing proper materials and detection systems. We believe that the HRS method has enormous potential for the application of pathogen detection, clinical analysis, and biomedical research.

Experimental Section

Gold nanoparticles with 15 nm diameter were synthesized by using a reported method.^[1a–d,q] In brief, aqueous solutions of $\text{HAuCl}_4 \cdot 3\text{H}_2\text{O}$ (0.01 %) and sodium citrate (1 wt %) were prepared. A solution of $\text{HAuCl}_4 \cdot 3\text{H}_2\text{O}$ (100 mL) was heated to reflux while being stirred. A solution of sodium citrate (3 mL, 1 %) was added to the boiling solution. The solution then underwent a series of color changes and finally turned wine red after which it was boiled for a further 30 min. After cooling to room temperature, the gold nanoparticle solution was diluted to 100 mL with deionized water. The gold nanoparticles were characterized by TEM (as shown in Figure 4) and were found to

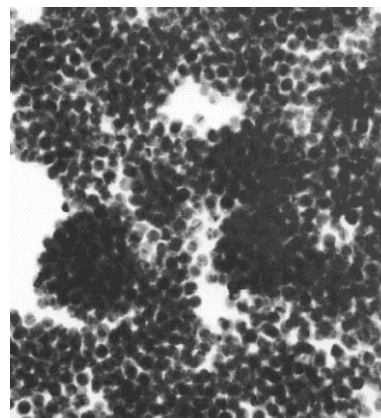


Figure 4. TEM image of aggregate gold nanoparticles after the addition of target DNA in probe DNA

be mostly spherical with the average diameter of 15 ± 3 nm. The UV/Vis absorption spectrum shows a well-developed surface plasmon absorption peak at 512 nm. Hybridization of the probe and the target was conducted for 5 minutes in PBS with NaCl (0.3 M) for a few minutes at room temperature. An aliquot of the hybridization solution was added to the gold colloid solution (1 mL), and PBS (1 mL) was then added immediately to the same solution. To estimate the number of DNA probes adsorbed on the gold nanoparticle surface, dithiothreitol was added to release the probes from the nanoparticles into solution. By using the ss-DNA quantification kit, we measured the concentration of the released DNA to be about

220 DNA probes per nanoparticle. To remove non-adsorbed probes, the solution was centrifuged at 13000 rpm for 20 min and the supernatant was replaced by buffer solution (2 mL). After another centrifugation under the same conditions, the precipitate was redispersed into the same buffer solution (1 mL) to make a stock solution, which was then used for the HRS experiments.

Received: September 2, 2005

Revised: November 24, 2005

Published online: January 11, 2006

Keywords: base pairs · DNA structures · hyper-Rayleigh scattering · nanostructures

-
- [1] a) N. L. Rosi, C. A. Mirkin, *Chem. Rev.* **2005**, *105*, 1547; b) P. Alivisatos, *Nat. Biotechnol.* **2004**, *22*, 47; c) M. Christine, D. Astruc, *Chem. Rev.* **2004**, *104*, 293; d) K. Kinbara, T. Aida, *Chem. Rev.* **2005**, *105*, 1377; e) I. Bontidean, A. Kumar, E. Csoregi, I. Yu, G. B. Mattiason, *Angew. Chem.* **2001**, *113*, 2748–2750; *Angew. Chem. Int. Ed.* **2001**, *40*, 2676; f) C. Dueymes, J. L. Decout, P. Peltie, M. Fontecav, *Angew. Chem.* **2002**, *114*, 504; *Angew. Chem. Int. Ed.* **2002**, *41*, 486; g) D. J. Maxwell, J. R. Taylor, S. Nie, *J. Am. Chem. Soc.* **2002**, *124*, 9606; h) H. Li, L. J. Rothberg, *Anal. Chem.* **2004**, *76*, 5414; i) W. C. Cao, R. C. Jin, C. A. Mirkin, *Science* **2002**, *297*, 1536; j) R. Nitu, Y. Li, *Angew. Chem.* **2005**, *117*, 5600; *Angew. Chem. Int. Ed.* **2005**, *44*, 5464; k) H. Shiigi, S. Tokonami, H. Yakabe, T. Nagaoka, *J. Am. Chem. Soc.* **2005**, *127*, 3280; l) H. Li, J. Huang, J. Lv, H. An, X. Zhang, Z. Zhang, C. Fan, J. Hu, *Angew. Chem.*, **2005**, *117*, 5230; *Angew. Chem. Int. Ed.* **2005**, *44*, 5100; m) K. Sato, K. Hosokawa, M. Maeda, *J. Am. Chem. Soc.* **2003**, *125*, 8102; n) B. Dubertrel, M. Calame, A. J. Libchaber, *Nat. Biotechnol.* **2001**, *19*, 365; o) H. Li, L. Rothberg, *Anal. Chem.* **2005**, *77*, 6229; p) P. C. Ray, A. Fortner, J. Griffin, C. K. Kim, J. P. Singh, H. Yu, *Chem. Phys. Lett.* **2005**, *414*, 259.
- [2] a) F. W. Vance, B. I. Lemon, J. T. Hupp, *J. Phys. Chem. B* **1998**, *102*, 10091; b) J. P. Novak, F. W. Vance, R. C. Johnson, B. I. Lemon, J. T. Hupp, D. L. Feldheim, *J. Am. Chem. Soc.* **2000**, *122*, 12029; c) P. Galleotto, P. F. Brevet, H. Girault, R. Antoine, M. Broyer, *J. Phys. Chem. B* **1999**, *103*, 8706; d) I. R. Antione, C. Jonin, J. Nappa, E. Benichou, P.-F. Brevt, *J. Chem. Phys.* **2004**, *120*, 10748; e) J. Nappa, G. Revillod, J. P. Abid, C. Jonin, E. Benichou, H. H. Girault, P. F. Brever, *Faraday Discuss.* **2004**, *125*, 145; f) C. Zhang, Y. Zhang, X. Wang, M. Tang, L.-Z. Hong, *Anal. Biochem.* **2003**, *320*, 136.
- [3] a) R. W. Terhune, P. D. Maker, C. M. Savage, *Phys. Rev. Lett.* **1965**, *14*, 681; b) K. Clays, A. Persoons, *Phys. Rev. Lett.* **1991**, *66*, 2980; c) C. Sporer, I. Ratera, Y. Zho, J. V. Gancedo, K. Wurst, P. Jaitner, K. Clays, A. Persoons, C. Rovira, J. Veciana, *Angew. Chem.* **2004**, *116*, 5378; *Angew. Chem. Int. Ed.* **2004**, *43*, 5266; d) J. J. Wolff, F. Siegler, R. Matschiner, R. Wortmann, *Angew. Chem.* **2000**, *112*, 1494; *Angew. Chem. Int. Ed.* **2000**, *39*, 1436; e) P. C. Ray, P. K. Das, *J. Phys. Chem.* **1995**, *99*, 17891.
- [4] a) B. J. Coe, L. A. Jones, J. A. Harris, B. S. Brunshawig, I. Asselberghs, K. Clays, A. Persoons, *J. Am. Chem. Soc.* **2004**, *126*, 3880; b) B. J. Coe, L. A. Jones, J. A. Harris, B. S. Brunshawig, I. Asselberghs, K. Clays, A. Persoons, *J. Am. Chem. Soc.* **2003**, *125*, 862; c) G. P. Bartholomew, I. Ledoux, S. Mukamel, G. C. Bazan, J. Zyss, *J. Am. Chem. Soc.* **2002**, *124*, 13480.
- [5] J. L. Oudar, *J. Chem. Phys.* **1977**, *67*, 446.
-